

Structural, Mechanical and Optical Properties of Plasma-chemical Si-C-N Films

A.O. Kozak, V.I. Ivashchenko, O.K. Porada, L.A. Ivashchenko, T.V. Tomila

Institute for Problems of Materials Sciences, NAS of Ukraine, 3, Krzhyzhanovsky Str., 03142 Kyiv, Ukraine

(Received 15 September 2014; published online 29 November 2014)

An influence of the substrate temperature in the range of 40-400 °C on the properties of the Si-C-N films deposited by plasma enhanced chemical vapor deposition (PECVD) technique using hexamethyldisilazane is analyzed. Study of the structure, chemical bonding, surface morphology, mechanical properties and energy gap of the obtained films was carried out using X-ray diffraction, infrared spectroscopy, X-ray photoelectron spectroscopy, atomic force microscopy, optical measurements and nanoindentation. It was established that all the films were X-ray amorphous and had low surface roughness. Intensive hydrogen effusion from the films takes place, when substrate temperature increases up to 400 °C, which promotes a decrease of roughness and an increase in hardness and Young modules more than twice.

Keywords: PECVD, Hexamethyldisilazane, Si-C-N films, FTIR, Nanoindentation.

PACS numbers: 81.15.Gh, 73.61.Jc, 62.20.Qp

1. INTRODUCTION

Ternary Si-C-N systems are a new kind of materials with unique properties inherited from silicon carbide and nitride. Thin Si-C-N films demonstrate high hardness (30 GPa), low coefficient of thermal expansion ($2.15 \times 10^{-6} / \text{K}$), high thermal (to temperatures over 1300 °C) and chemical stability [1-3], such that they can be used as wear-resistant and protective coatings. Due to the possibility of control of the energy gap width [4, 5], Si-C-N materials are promising semiconductors.

Si-C-N films are currently obtained by many different chemical and physical methods, such as CVD [6], PECVD [4, 7-9], vapor-transport CVD [5], magnetron sputtering [10, 11], ion or plasma spraying [12], ion implantation [13, 14], etc. that confirms a great interest to them.

The aim of the present work was to investigate the influence of one of the main parameters of plasma enhanced chemical vapor deposition (PECVD), namely, the substrate temperature on the properties of Si-C-N films deposited from non-traditional and inexpensive domestic precursor – hexamethyldisilazane (HMDS, $(\text{CH}_3)_6\text{Si}_2\text{NH}$), whose molecules contain all the necessary components for the formation of Si-C-N films. Studies of the films deposited from HMDS are still in embryo state.

2. DETAILS OF THE EXPERIMENT

Si-C-N films were deposited by the PECVD method on the laboratory plant of a planar type with a capacitive plasma excitation system. Gas discharge in the working chamber was excited by RF generator of 40.68 MHz. Bias potential on the substrate was provided by an additional RF generator. Liquid precursor HMDS was used as the main agent. HMDS vapor was transported from thermostated bubbler heated to 40 °C into the reactor chamber using hydrogen. The films were deposited on silicon substrates. Directly before deposition silicon substrates were etched in 10 % solution of hydrofluoric acid, and then cleaned by etching in hydrogen plasma.

The films were deposited at the substrate-holder temperatures of 40, 120, 200, 300 and 400 °C and the following constant parameters: the bias on the substrate $U_s = -200$ V, pressure of the working gas mixture in

reactor $P_c = 0.2$ Torr, discharge power from the main RF generator $P_w = 0.2$ W/cm³, hydrogen flow through the thermostated bubbler with HMDS FH + HMDS = 12 cm³/min. Deposition time is 60 min.

The X-ray diffraction (XRD) investigations were performed using the diffractometer “DRON-3M”. The study of the picture of chemical bonding was carried out by the Fourier transform infrared spectroscopy (FTIR) and X-ray photoelectron spectroscopy (XPS). The FTIR spectra were measured in the wavenumber range of 400-4000 cm⁻¹ on the spectrometer “FSM 1202” (LTD Infra-spec). The XPS spectra were obtained by using “UHV-Analysis-System, SPECS” (Germany) equipped by semi-spherical analyzer PHOIBOS-150. The film surface was analyzed on the atomic-force microscope “NanoScope IIIa Dimension 3000TM”. Nanoindentation was performed using the device G 200 equipped by the Berkovich indenter. Nanohardness (H) and modulus of elasticity (E) by the nanoindentation results were calculated by the Oliver and Farr method [15]. The film thickness was determined on the interference profilometer “Micron-alfa” (Ukraine). The optical energy gap is estimated from the measurements of the optical absorption spectra on the device SPECORD-M40 by using the Tauc relation $\alpha h\nu = A(h\nu - E_g)^{1/2}$, where α is the transmission coefficient; $h\nu$ is the photon energy; E_g is the optical energy gap; A is the coefficient of proportionality which does not depend on the photon energy [16].

3. EXPERIMENTAL RESULTS AND DISCUSSION

The film thickness was equal to 0.6-1.6 μm. The maximum values of the film thickness, namely, ~ 1.6 μm are achieved for the films deposited at the temperature of 40 °C. With increasing temperature above 100 °C, thickness depends weakly on the temperature change and is equal to ~ 0.7 μm.

The XRD patterns represented in Fig. 1 indicate the absence of any crystalline phase. This implies that the obtained films are X-ray amorphous (a-Si-C-N films). The peaks appearing at 33°, 62°, 69° correspond to the substrate material.

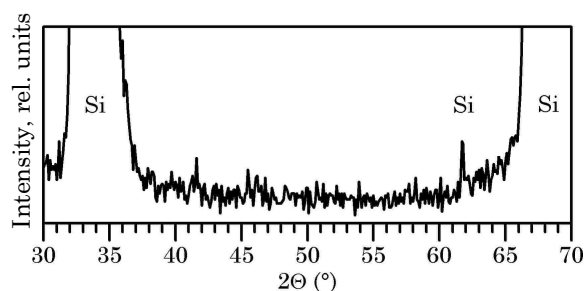


Fig. 1 – X-ray diffraction pattern of the Si-C-N films obtained by the PECVD technique from hexamethyldisilazane at the substrate-holder temperature of $T_s = 300^\circ\text{C}$

The FTIR spectra of the Si-C-N films deposited at the substrate-holder temperatures of 40°C , 300°C and 400°C are illustrated in Fig. 2. They are characterized based on the literature data of [4, 8, 17-19]. A general view of the spectra indicates the presence of a wide absorption region in the range of $600\text{--}1200\text{ cm}^{-1}$, which can be represented by a combination of several absorption bands and also vibration bands of the C-C bonds at 1550 cm^{-1} [19] and hydrogen bonds Si-H [20], C-H [4] and N-H [8, 20] at 2130 cm^{-1} , 2877 cm^{-1} and 3375 cm^{-1} , respectively. Hydrogen bands decrease with increasing temperature.

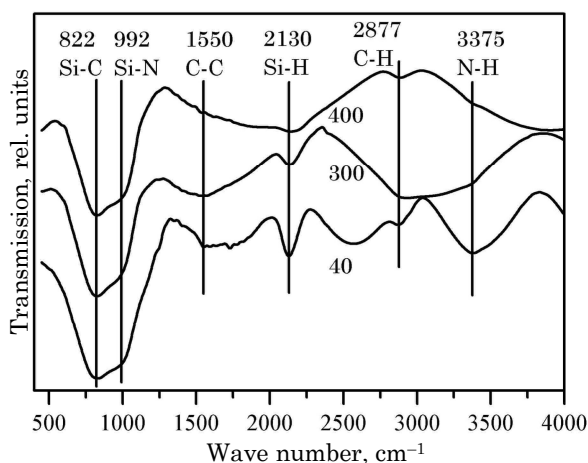


Fig. 2 – FTIR spectra of the Si-C-N films deposited at different substrate-holder temperatures

The dominant wide absorption band can be interpreted as a set of vibrations of Si-C ($650\text{--}850\text{ cm}^{-1}$) [21, 22], Si-N ($850\text{--}990\text{ cm}^{-1}$) [23, 5, 8] and Si-O ($1000\text{--}1030\text{ cm}^{-1}$) [18] bonds which prevail in the given range. Vibrations of hydrogen Si-H [8] and C-H [5] bonds with the peaks near 870 cm^{-1} and 990 cm^{-1} , which give an insignificant contribution to a wide absorption band, are also present in this range. Decrease in the intensity of a wide absorption band with increasing temperature is induced by a continuous hydrogen effusion from the film.

Despite the fact that with increasing temperature hydrogen bonds at 2130 cm^{-1} , 2877 cm^{-1} and 3375 cm^{-1} have a tendency to decrease in the absorption intensity, their redistribution also occurs. The results of the FTIR spectroscopy imply that with increasing temperature to 300°C , destruction of Si-H and N-H bonds takes place, and released in this case hydrogen forms new C-H bonds. Decrease in the vibration intensity of the C-H bonds at

$T_s > 300^\circ\text{C}$ indicates that at temperatures near 300°C C-H bond breaking starts. Simultaneous decrease in the absorption intensity of all the absorption peaks connected with hydrogen is observed at 400°C .

Further analysis of the picture of chemical bonding is performed using the XPS. XPS of Si2p, C1s, N1s and O1s levels of the films deposited at the substrate holder temperatures of 40°C and 300°C is shown in Fig. 3. All the spectra are shifted towards lower binding energies with increasing temperature. Decrease in the intensity of Si2p, N1s and O1s photoelectron peaks and increase in C1s photoelectron peak takes place simultaneously. Position of the peaks of the XPS spectra clearly implies the presence of the Si-N [21], C-C [24], N-C [25] and O-Si [20] bonds.

Decomposition of the XPS spectra to the Gaussian components (Fig. 3) gave the possibility to specify the changes of the pattern of chemical bonding in the films. Si2p peak is represented in the form of three Gaussian components with the vertices at 103.0 eV , 101.7 eV and 100.5 eV which are ascribed to the Si-C (100.5 eV) [5, 24] bonds in SiC, Si-N (101.7 eV) [26, 27] bonds in Si_3N_4 and Si-O (103 eV) [8] bonds. Temperature increase leads to the shift of the Si-C peak towards lower energies and insignificant increase in its intensity, as well as to the decrease in the Si-N and Si-O peaks. XPS C1s spectra are also represented by three components with the centers at 283.2 eV , 284.8 eV and 286.8 eV which correspond to the C-Si bonds [5], C-C bonds in SiC [17] and C-N bonds [25], respectively.

Hydrogen C-H bonds [28], which are manifested with the values of the binding energy of 284.5 eV , 285 eV , 286.5 eV , can contribute to all decomposed components. Increase in the photoelectron peak C1s with increasing temperature to 300°C occurs, mainly, due to the increase in the C-C and C-H bonds. Temperature increase also leads to the shift of the C-N bonds peak towards lower energies. In this case, a general behavior of the distribution remains almost constant.

N1s spectra represented by three peaks localized at 397.8 eV , 398.6 eV , 400.1 eV belong to the N-Si bonds ($397.1\text{--}397.8\text{ eV}$) in Si_3N_4 [16, 28] and N-C sp^3 bonds in C_3N_4 ($398.3\text{--}400.3\text{ eV}$) [25, 29, 30]. Increase in the substrate-holder temperature leads to the increase in the N-Si peak on account of the decrease of the N-C sp^3 bonds peak. Finally, XPS O1s spectra were divided into two Gaussian components with the centers at 531.6 eV and 532.8 eV . These components are connected with the O-C and O-Si [31] bonds, respectively, distribution of which is not changed with increasing temperature, but a considerable decrease in the photoelectron peak takes place. The presence of this peak can be induced by both the films oxidation during their storage and presence of oxygen in the initial film components.

Picture of chemical bonding obtained from the XPS investigations agrees with the results obtained by the FTIR spectroscopy and indicates that Si-N, Si-C, C-N, C-C and Si-O bonds make the main contribution in the obtained films. It was observed that the increase in the substrate holder temperature leads to the strengthening of the Si-C and C-C bonds and weakening of the Si-N, C-N and O-Si bonds and hydrogen bonds as well.

We have estimated the film composition by the XPS spectra. The results indicate that the increase in the

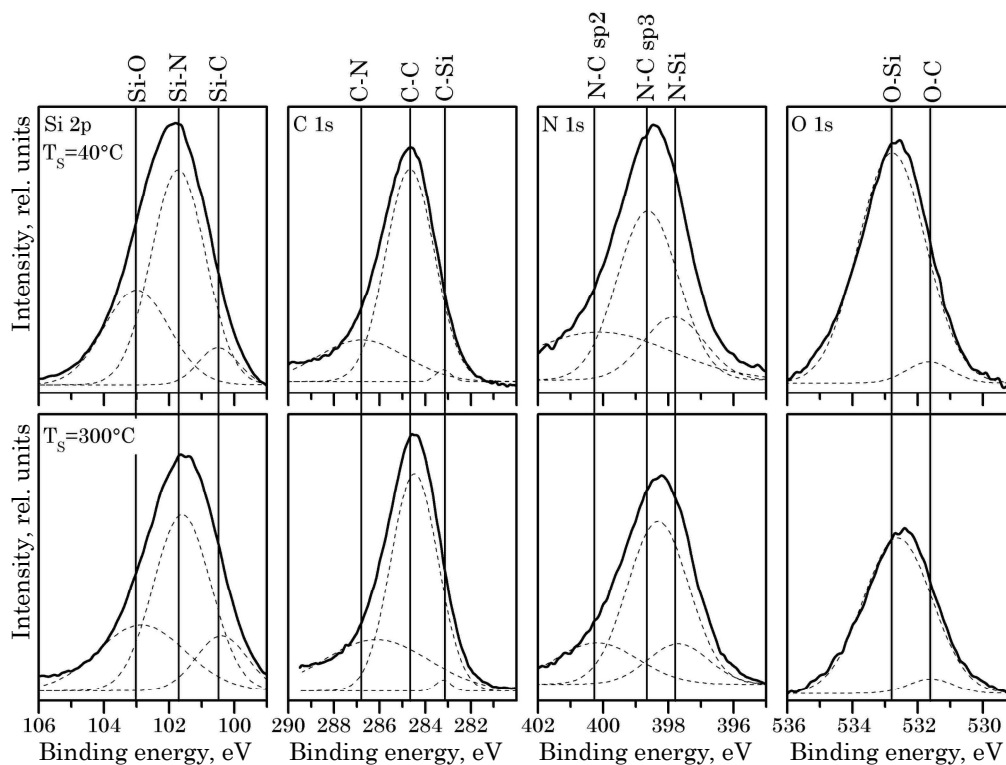


Fig. 3 – Gaussian components of the XPS spectra of the main levels of the deposited films

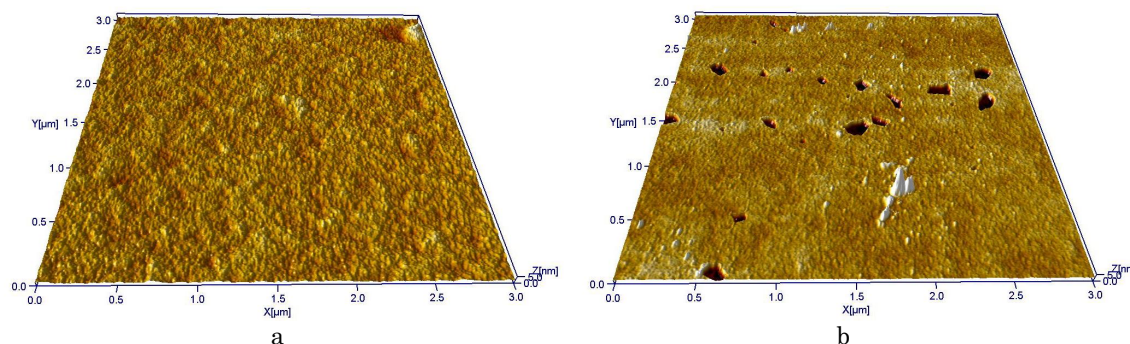


Fig. 4 – AFM-images of the surface of the Si-C-N films deposited at $T_s = 40\text{ }^{\circ}\text{C}$ (a) and $T_s = 400\text{ }^{\circ}\text{C}$ (b)

amount of C from 47 at. % to 53 at. % and the decrease in the content of Si, N, O from 31, 11, 11 at. % to 8, 10, 29 at. %, respectively, occur with the increase in the substrate-holder temperature from $40\text{ }^{\circ}\text{C}$ to $400\text{ }^{\circ}\text{C}$.

Study of the surface morphology of the obtained Si-C-N films was carried out using AFM. The AFM images for the films deposited at $40\text{ }^{\circ}\text{C}$ and $400\text{ }^{\circ}\text{C}$ are shown in Fig. 4. The determined value of the root-mean-square (RMS) roughness for the films deposited at $40\text{ }^{\circ}\text{C}$ is equal to 0.5 nm, while for the films deposited at $400\text{ }^{\circ}\text{C}$ – $\text{RMS} = 0.2\text{ nm}$.

The characteristic feature of two AFM images is the fact that surface of the films deposited at different values of the substrate temperature is sufficiently uniform and does not have special relief differences that confirms the results of the XRD analysis about the absence of crystalline inclusions in the obtained films. Decrease in the roughness is induced by the reduction in the hydrogen content in the films that leads to the compaction of the

films with the decrease in their porosity that, in turn, leads to the decrease in the roughness more than twice.

Mechanical properties of the Si-C-N films were studied by nanoindentation (Fig. 5). The nanoindentation results illustrated in Fig. 5 taken at different substrate-holder temperatures show the distribution of nanohardness and modulus of elasticity on the indenter penetration depth. With increasing temperature from $40\text{ }^{\circ}\text{C}$ to $400\text{ }^{\circ}\text{C}$ nanohardness increases from 8 to 19 GPa, and here, the modulus of elasticity also increases from 75 to 150 GPa. When reaching $400\text{ }^{\circ}\text{C}$, a tendency to further increase in the hardness is observed. The same tendency takes also place for the dependence of the modulus of elasticity on the substrate-holder temperature.

H/E ratio for the films obtained at $400\text{ }^{\circ}\text{C}$ is equal to 0.13 and indicates that the given films should demonstrate good tribological properties.

Such change in the hardness can be explained based on the FTIR and XPS techniques using the theoretical

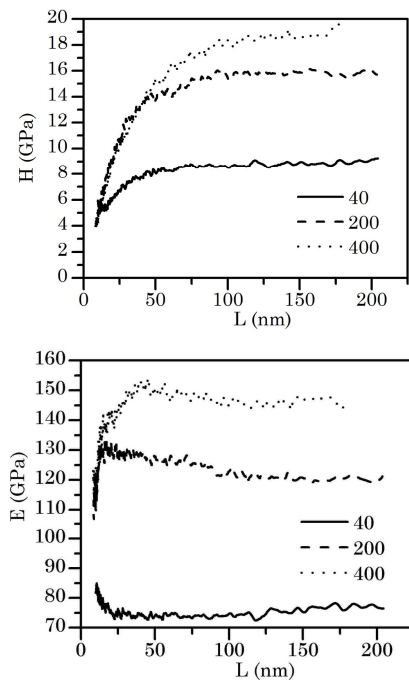


Fig. 5 – Distribution of the nanohardness and modulus of elasticity on the indenter penetration depth

and experimental results. Due to the hydrogen and oxygen effusion and the increase in the amount of more ordered Si-C bonds, compaction of the films occurs that, in turn, leads to the increase in the hardness of the obtained Si-C-N films.

Energy gap is one of the parameters characterizing amorphous semiconductors. The energy gap value of the obtained films was estimated by the Tauc correlation (see Fig. 6a) from the absorption spectrum illustrated in Fig. 6b, extrapolation of the linear section of the dependence $(\alpha h\nu)^{1/2}$ to $\alpha = 0$, and was equal to 1.4 eV. We assume that the given energy gap separates the “traces” of the valence band and the conduction band. The obtained understated values of the energy gap are connected with a large amount of the C-C carbon bonds in the films [32], but are in a wide range of the optical energy gaps corresponding to amorphous Si-C-N films (0.96-4.3 eV) [16].

4. CONCLUSIONS

1. Si-C-N films were deposited by the PECVD technique from hexamethyldisilazane.

REFERENCES

1. Z.L. Sun, Y. Zhou, et al., *Mater. Lett.* **72**, 57 (2012).
2. B.P. Swain, N.M. Hwang et al., *Appl. Surf. Sci.* **254**, 5319 (2008).
3. C. Pusch, H. Hoche, *Surf. Coat. Technol.* **205**, S119 (2011).
4. T.P. Smirnova, A.M. Badalina, et al., *Thin Solid Films* **429**, 144 (2003).
5. Y. Awad, M.A. El Khahani, et al., *J. Appl. Phys.* **107**, 033517 (2010).
6. A. Bendeddouche, R. Berjoan, et al., *Surf. Coat. Technol.* **111**, 184 (1999).
7. D. Kuo, D. Yang, *Thin Solid Films* **374**, 92 (2000).

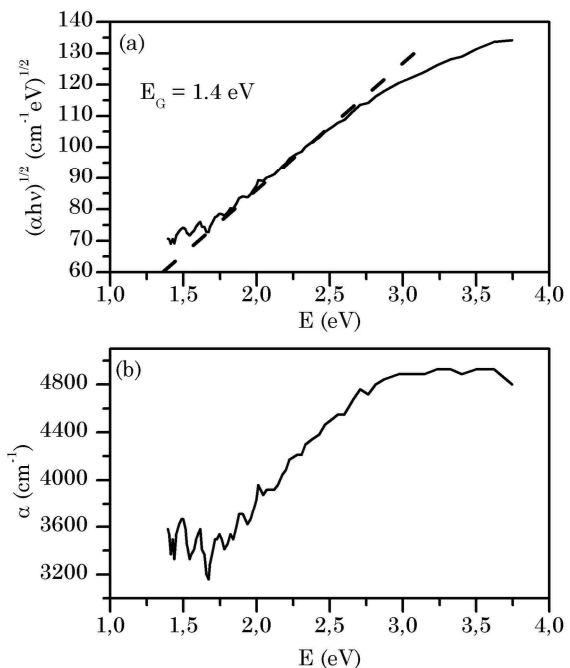


Fig. 6 – The Tauc function $(\alpha h\nu)^{1/2}$ (a) and typical optical absorption spectrum (b) of the deposited Si-C-N films

2. Si-C-N films are X-ray amorphous for the substrate-holder temperatures from 40 °C to 400 °C and demonstrate a low surface roughness.

3. Si-C, Si-N and C-N bonds are the main bonds in the films. Increase in the substrate temperature leads to the decrease in the number of hydrogen C-H, Si-H and N-H bonds.

4. Effusion of hydrogen and oxygen with increasing deposition temperature promotes the compaction of the films that, in turn, leads to the increase in their hardness and modulus of elasticity.

5. Optical energy gap of the deposited films is equal to 1.4 eV.

6. The results obtained in the given work allow to recommend Si-C-N films for use in microelectronic mechanical systems.

ACKNOWLEDGEMENTS

This work has been performed under the Project STCU No5964. The authors of the paper express deep gratitude to S.N. Dub, O.S. Lytvyn, I.I. Timofeeva and O.Yu. Khyzhun for the conducted investigations of the obtained samples.

8. P. Jedrzejowski, J. Cizek, et al., *Thin Solid Films* **447-448**, 201 (2004).
9. J. Huran, A. Valovič, et al., *J. Electrical Eng.* **63**, 333 (2012).
10. Z. Shi, Y. Wang, et al., *Appl. Surf. Sci.* **258**, 1328 (2011).
11. V.M. Ng, M. Xu, et al., *Thin Solid Films* **506-507**, 283 (2006).
12. N.V. Novicov, M.A. Voronkin, et al., *Diamond Related Mater.* **1**, 580 (1992).
13. C. Uslu, B. Park, D.B. Poker, *J. Electron. Mater.* **25**, 23 (1996).
14. Y. Liu, X. Zhang, et al., *Thin Solid Films* **518**, 4363 (2010).
15. W.C. Oliver, G.M. Pharr, *J. Mater. Res.* **7** No6, 1564 (1992).

16. I.V. Afanasyev-Charkin, M. Nastasi, *Surf. Coat. Technol.* **199**, 38 (2005).
17. X.B. Yan, B.K. Tay, et al., *Electrochem. Commun.* **8**, 737 (2006).
18. M. Xu, S. Xu, et al., *J. Non-Cryst. Solids* **352**, 5463 (2006).
19. Ferreira, E. Fortunato, et al., *J. Non-Cryst. Solids* **352**, 1361 (2006).
20. D. Sarangi, R. Sanjinés, A. Karimi, *Thin Solid Films* **447-448**, 217 (2004).
21. W. Besling, A. Goossens, et al., *J. Appl. Phys.* **83**, 544 (1998).
22. N.I. Fainer, M.L. Kosinowa, Y.M. Romyantsev, *Russ. Chem. J.* **45** No3, 101 (2001).
23. Y. Awad, M.A. El, et al., *Surf. Coat. Technol.* **204**, 539 (2009).
24. M.E Ramsey, E. Poindexter, et al., *Thin Solid Films* **360**, 82 (2000).
25. X.-C. Xiao, Ya-W. Li, et al., *Appl. Surf. Sci.* **156**, 155 (2000).
26. X. Peng, L. Song, et al., *J. Vac. Sci. Technol. B* **20**, 159 (2002).
27. Bendeddouche, R. Berjoan, et al., *J. Appl. Phys.* **81**, 6147 (1997).
28. T.P. Smirnov, A. Badalyan, *VII ISTAPC*, 3 (2005).
29. K. Yamamoto, Y. Koga, S. Fujiwara, *Diamond Related Mater.* **10**, 1921 (2001).
30. S. Ma, B. Xu, et al., *Surf. Coat. Technol.* **202**, 5379 (2008).
31. A. Majumdar, G. Das, et al., *J. Electrochem. Soc.* **155** No1, D22 (2008).
32. V.I. Ivashchenko, A.O. Kozak, O.K. Porada, et al., *Thin Solid Films* **569**, 57 (2014).